Water Air Soil Pollut (2019) 230: 67
https://doi.org/10.1007/s11270-019-4115-z

Pyrene Degradation by *Mycobacterium gilvum*: Metabolites and Proteins Involved

Fengji Wu · Chuling Guo · Shasha Liu · Xujun Liang · Guining Lu · Zhi Dang

Received: 5 December 2018 / Accepted: 4 February 2019 / Published online: 22 February 2019

Abstract Polycyclic aromatic hydrocarbons (PAHs) are toxic organic pollutants and omnipresent in the aquatic and terrestrial ecosystems. A high-efficient pyrene-degrading strain CP13 was isolated from activated sludge and identified as *Mycobacterium gilvum* based on the analysis of 16S rRNA gene sequence. More than 95% of pyrene (50 mg L^{-1}) was removed by CP13 within 7 days under the alkaline condition. Pyrene metabolites, including 4-phenanthrenecarboxylic acid, 4-phenanthrenol, 1-naphthol, and phthalic acid, were detected and characterized by GC-MS. Results suggested that pyrene was initially attacked at positions C-4 and C-5, then followed by *ortho* cleavage, and further degraded following the phthalate metabolic pathway. Analysis of pyrene-induced proteins showed that the extradiol dioxygenase, a key enzyme involved in pyrene degradation, was highly up-regulated in pH 9 incubation condition, which illustrated the high efficiency of CP13 under alkaline environment. The present study demonstrated that the isolated bacterial strain CP13 is a good candidate for bioremediation of alkaline PAH-contaminated sites.

Keywords Alkaline environment · Biodegradation · Metabolites · *Mycobacterium* · Protein expression · Pyrene

F. Wu · C. Guo (✉) · G. Lu · Z. Dang
School of Environment and Energy, South China University of Technology, Guangzhou 510006, China
e-mail: clguo@scut.edu.cn

C. Guo · G. Lu · Z. Dang
The Key Lab of Pollution Control and Ecosystem Restoration in Industry Clusters, Ministry of Education, South China University of Technology, Guangzhou 510006, China

S. Liu
School of Environmental and Chemical Engineering, Zhaoqing University, Zhaoqing 526061, China

X. Liang
Guangdong Key Laboratory of Environmental Pollution and Health, and School of Environment, Jinan University, Guangzhou 510632, China

1 Introduction

Polycyclic aromatic hydrocarbons (PAHs) are toxic organic pollutants and omnipresent in the environment, imposing detrimental effects on the ecosystems and public health because of their carcinogenicity, teratogenicity, and mutagenicity (Zhong et al. 2006; Liu et al. 2017; Kumari et al. 2018). They are mostly generated from incomplete combustion of organic compounds (e.g., crude oils and coal) and emitted into the surface waters and sediments primarily via industrial activities (e.g., fossil fuel refining processes) (Chen et al. 2015; Kristanti et al. 2018). Microbial transformation and degradation have been regarded as one of the effective and practical methods for PAH elimination in both aquatic and terrestrial ecosystems (Guo et al. 2010; Liu et al. 2016). So far, significant influences of environmental parameters (e.g., pH and temperature) on PAH degradation have been documented. The variation of pH is related to the processes of production and the

characteristics of industrial waste or sewage, which may consequently lead to soil alkalization/acidification (Smol and Wlodarczyk-Makula 2012; Zhang et al. 2013). However, most of the research showed that pyrene-degrading bacterial strains were effective within the neutral condition (pH 6.5–7.5) (Table 1), and those that remain highly efficient under alkaline condition are rare.

Pyrene, composed of four fused benzene rings, has been selected as a typical compound because of the structural similarity of some carcinogenic PAHs (Mukherjee et al. 2017; Balcom and Crowley 2010). To date, pyrene degradation pathway by *Mycobacterium* species has been proposed extensively and been considered to be stimulated by a series of enzymes, and two major pathways have been well documented: (i) The initial oxidation reaction takes place in positions C-1 and C-2 of pyrene (i.e., pyrene-1,2-diol) and generates an *O*-methylated metabolite afterwards; (ii) positions C-4 and C-5 (K region) of pyrene are initially oxidized to form 4,5-dihydroxypyrene which is followed by *ortho* cleavage, then decarboxylated, and further oxidized to lesser ringed intermediate products, such as 4-phenanthrenecarboxylic acid and 4-phenanthrol (Liang et al. 2006; Krivobok et al. 2003; Kim et al. 2007; Seo et al. 2011; Kweon et al. 2011). Regarding the proteins involved in pyrene degradation process, the expression level changes correspondingly with external conditions as a result of adaptive responses (Kim et al. 2004). Molecular studies on protein expression that relevant to the activities of key enzymes corresponding to pyrene induction and pH adaptation contribute to the progression of feasible bioremediation applications (Badejo et al. 2013a, b). Investigation of proteins that induced under different conditions provides a better understanding of pyrene degradation mechanisms as well as the adaptive responses of microorganisms.

In this study, a bacterial strain with high efficiency of pyrene degradation was isolated from activated sludge and identified as *Mycobacterium gilvum* strain CP13. Incubation conditions (i.e., initial pyrene concentration, temperature, and pH) that affect the degradation efficiency were investigated. Moreover, metabolites produced in the degradation process were detected and characterized by gas chromatography-mass-spectrometry (GC-MS). Pyrene-induced proteins were separated by two-dimensional gel electrophoresis (2-DE), and the up-regulated proteins were further identified as well. This study will provide a basic understanding of pyrene biodegradation under alkaline condition, which is a solid foundation for bioremediation of PAH-contaminated environment.

2 Materials and Methods

2.1 Chemicals and Culture Media

The activated sludge was obtained from a coking wastewater treatment plant of SGIS Songshan Co., Ltd.,

Table 1 Comparisons of pyrene degradation incubation conditions and degradation efficiency

Strain	Incubation conditions			Time	Degradation	References
	Initial concentration	pH	Temperature (°C)			
CP13	50 mg L^{-1}	8–9	35	7 days	>95%	This study
Pseudomonas monteilii PL5	20 mg L^{-1}	6	35	10 days	56.5%	Ping et al. (2017)
Pseudomonas sp. W10	200 mg L^{-1}	7	37	30 days	20%	Chebbi et al. (2017)
Hydrogenophaga sp. PYR1	20 mg L^{-1}	9	28	15 days	94%	Yan et al. (2017)
Thalassospira sp. strain TSL5–1	20 mg L^{-1}	7.4	30	25 days	42.5%	Zhou et al. (2016)
Acinetobacter strain USTB-X	100 mg L^{-1}	7	30	16 days	63%	Yuan et al. (2014)
Klebsiella pneumonia PL1	20 mg L^{-1}	7	40	10 days	63.4%	Ping et al. (2014)
Microbacterium sp. strain BPW	100 mg L^{-1}	6.5–7	30	14 days	71.7%	Wongwongsee et al. (2013)
Mycobacterium gilvum PYR-GCK	25 μM	6.5	30	48 h	100%	Badejo et al. (2013a)
Bacillus vallismortis strain JY3A	150 mg L^{-1}	7	37	15 days	70%	Ling et al. (2011)
Mycobacterium sp. strain MHP-1	0.1% (*w*/*v*)	9	30	7 days	50%	Habe et al. (2004)

China. Pyrene (purity ≥ 98%) was brought from Sigma-Aldrich Chemical Company. Other chemicals were purchased from Guangzhou Chemical Reagent Factory (China) and of the highest purity. The acetone (redistilled) was used as solvent in the preparation of pyrene stock solution (5 g L^{-1}). The mineral salt medium (MSM) was used as culture media for the pyrene-degrading strain. The components of MSM were modified from Guo et al. (2010) and listed as follows (per liter): $(NH_4)_2SO_4$, 100 mg; $MgSO_4{\cdot}7H_2O$, 20 mg; $CaCl_2{\cdot}2H_2O$, 10 mg. Trace elements were composed of $FeSO_4{\cdot}7H_2O$, 1.2 mg; $MnSO_4{\cdot}H_2O$, 0.3 mg; $ZnSO_4{\cdot}7H_2O$, 0.3 mg; $CoCl_2{\cdot}7H_2O$, 0.1 mg; $(NH_4)_6Mo_7O_{24}{\cdot}4H_2O$, 0.1 mg. The potassium phosphate buffer (0.02 M) was utilized to dissolve the chemicals of MSM with pH 7.4. By adding 2% agar into the MSM solution, the MSM agar plates were made. Deionized water was involved in the whole study.

2.2 Enrichment and Isolation

The activated sludge was used as inoculum. An adequate volume of pyrene stock solution (0.5 mL) was added to a sterilized conical flask (150 mL) to serve as the unique carbon and energy source. After the solvent evaporated, 45 mL MSM, as well as 5 mL inoculum, was added to the flask. The final concentration of pyrene was 50 mg L^{-1}. Then, the flask was placed in the dark and shaken at 150 rpm for 7 days at 30 °C (Hilyard et al. 2008). Additional culture flask without inoculum was set as negative control. Afterwards, 5 mL cultured liquid was regularly transferred to a fresh flask with 45 mL MSM containing pyrene (50 mg L^{-1}). After five times' transformation, enrichment kept stable with turbidity compared with the control. Then, 0.1 mL of dilute cultured liquid was spread on an MSM agar plate with surficial pyrene for isolation. The bacterial colonies surrounded by clarified zones were purified by the nutrient agar plates and then subcultured to the liquid MSM with pyrene.

2.3 Identification of Strain

The isolated pyrene-degrading strain was investigated by morphology observation, Gram staining, and 16S rRNA gene partial sequence analysis. Cells grown on nutrient broth (NB) ager plate were prepared for DNA extraction which was done by the DNA extraction kit following the instructions of the manufacturer. The final extracted DNA was resuspended in TE buffer and visualized in agarose gels (1%) according to standard procedures. The DNA suspension was placed at − 20 °C before utilization. The fragment of DNA was amplified using an S1000TM Thermal Cycler PCR System (Bio-Rad, USA) with primers of 27F (AGAGTTTG ATCCTGGCTCAG) and 1492R (TACCTTGT TACGACTT). The PCR amplification procedure was initially incubated at 94 °C for 3 min, then following the thermal cycling program (for a total of 35 cycles): 94 °C for 0.5 min of denaturation, 55 °C for 0.5 min of primer annealing, and 72 °C for 1.5 min of chain extension and adjusted with an extension time of 5 min in the last cycle. The sequence similarity analysis was performed in the NCBI database using BLAST program. The neighbor-joining (NJ) phylogenetic tree was performed by the program MEGA (version 6.0) (Yan et al. 2017). The 16S rRNA gene partial sequence of CP13 was uploaded to the online database (GenBank) with an accession number of KF378755.

2.4 Pyrene Biodegradation

After pre-cultivation to the exponential phase in MSM containing pyrene in the dark, cells were centrifuged, then washed twice using potassium phosphate buffer and resuspended in MSM adjusting to an OD_{600} of 0.5 as inoculum. Flasks with 18 mL MSM containing 25, 50, 75, 100, and 150 mg L^{-1} of pyrene were inoculated 2 mL inoculum then incubated for 7 days at 30 °C in the dark. The following experiments were performed under the optimum pyrene concentration (50 mg L^{-1}). Effects of temperatures (25, 30, 35, 40, and 45 °C) and pH (5, 6, 7, 8, 9, and 10) on pyrene degradation efficiency were examined. Non-inoculated flasks were used as abiotic controls, and each treatment was set in triplicate.

The residual pyrene was extracted as described by Zhang and Zhu (2009) with slight modifications. Adequate methanol (HPLC grade) was added into the sample flasks and then placed into ultrasonic washing machine until the pyrene was dissolved completely. Afterwards, the dissolved solutions were transferred into volumetric flasks and diluted with methanol. Samples were analyzed by HPLC (Agilent 1200 series) with a reverse phase C18 column (4.6 × 150 mm) after filtration (a 0.22-μm filter). The mobile phase of methanol-water mixture (*v*/*v*, 95/5) was set at a flow rate of 1 mL min^{-1}, and the absorption wavelength of UV was 234 nm.

Differences in pyrene degradation activities were confirmed using one-way analysis of variance (ANOVA) with Tukey's HSD-post hoc test ($\alpha < 0.05$).

2.5 Detection of Pyrene Metabolites

To identify pyrene degradation byproducts, cells were pre-cultivated in MSM with pyrene (50 mg L^{-1}) for 1, 3, 5, and 7 days, respectively. The metabolite extraction was followed the procedure described by Lu et al. (2013). The extracts were dissolved using dichloromethane with a final volume of 100 μL. A volume of 3 μL metabolite sample was injected to GC-MS (DSQ II, Thermo Fisher) with a column of 30 m × 0.25 mm at 100-kPa helium pressure. The temperature of GC oven was performed as follows: firstly, set at 70 °C held for 5 min, then gradually raised to 200 °C by 15 °C min^{-1}, then to 280 °C by 5 °C min^{-1}, and then finally to 300 °C by 10 °C min^{-1} and held for 5 min.

2.6 Protein Extraction

All cells were harvested by centrifugation after incubation. Each 20-mg cell pellets were resuspended by adding 150–200-μL Alklysis buffer containing 20 mM Tris, 2 M thiourea (Amersham Biosciences), 6 M urea (Amersham Biosciences), 1 mM PMSF, 20 mM DTT, and 2% (*w*/*v*) CHAPs (Usb), and then frozen at −80 °C for 2 days. Afterwards, cells were placed in an ultrasonic crasher for homogenization at 4 °C for 5 min until the supernatant was transparent. The crude protein extracts were collected after removing the cell debris and insoluble materials by centrifugation for 10 min (4 °C, 12,000 rpm). The protein purification was completed by Ready prep 2-D cleanup kit (Bio-Rad, USA), and the content measurement was analyzed by Bio-Rad protein assay. The protein samples were stored at − 80 °C before utilization.

2.7 Protein Separation and Identification

Protein separation and peptide sequence analysis were conducted at Guangzhou Jinfeng Biotechnology Co. Ltd. (China). Each protein sample (300 μg) was mixed with rehydration buffer composed of 20 mM DTT, 2 M thiourea, 0.5% (*v*/*v*) IPG buffer, 7 M urea and 2% (*w*/*v*) CHAPs, and then loaded on the Immobiline DryStrips (17 cm, pH 4 to 7). The rehydration and isoelectric focusing were carried out on an Ettan IPGphor3 (Amersham Biosciences). The program of isoelectric focusing was as follows (a total of 52,000 Vh): 30 min at 300 V, 30 min at 700 V, 1.5 h at 1500 V, 3 h at 8000 V, and 4 h 8000 V. The proteins were separated on prefabricated polyacrylamide criterion gels (15%) ranging from 10 to 130 kDa. Afterwards, the strip equilibration was held within DTT and IAA in SDS equilibration buffer, and then transferred to the criterion gels. The second-dimension electrophoresis was performed in Ettan DalTsix (Amersham Biosciences) initially at 10 mA for 1 h and then increased to 38 mA for about 5 h. Proteins were stained by silver for visualization after electrophoresis.

The images of gels were made by UMAX scanner and analyzed by PDQuest 2D Analysis Software version 8.0.1 (Bio-Rad, USA). The proteins were identified if the abundance of pyrene-treated samples was found to be considerably increased by twofold or more in comparison with the non-pyrene-treated sample. The substrate for non-pyrene-treated sample was sorbitol, since its catabolism is not related to the pyrene metabolic pathway (Kim et al. 2007). The analysis of peptide sequences of selected protein spots was detected by Ultraflex III MALDI-TOF/TOF-MS (Bruker, German), following the protocol suggested by the manufacturer. The peptide sequences were then searched on the Mascot website (http://www.matrixscience.com) and compared with those in NCBInr databases.

3 Results and Discussion

3.1 Isolation and Identification of Pyrene-Degrading Strain

The pyrene-degrading strain CP13 was isolated from the activated sludge collected from a treatment plant for coke-oven wastewater. The bacterial colony of CP13 was yellow, smooth, convex, opaque, and wet. This bacterium is Gram-positive, short rod (about 0.4–0.7 μm), non-sporulating, and aerobic. According to the 16S rRNA gene partial sequence (1408 bp) of strain CP13, a phylogenetic tree was constructed which gives a better comparison between CP13 and other highly similar strains (Fig. 1). The sequence alignment indicated that strain CP13 was closely related with genus *Mycobacterium* and was over 99% similarity to *Mycobacterium gilvum* strain YSP1-1 (JF894167), *Mycobacterium gilvum PYR-GCK* (CP000656), and

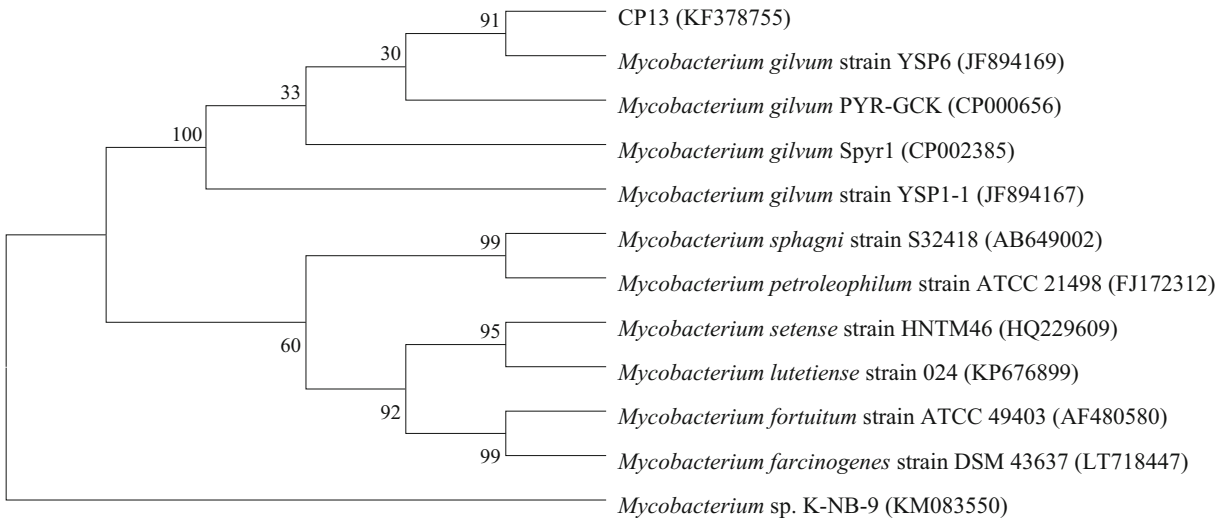

Fig. 1 Phylogenetic tree of strain CP13 based on 16S rRNA gene fragment sequence with neighbor-joining method by using program MEGA (Version 6.06)

Mycobacterium gilvum Spyr1 (CP002385). Therefore, the strain CP13 could be classified as *Mycobacterium gilvum*.

Besides the fact that the presence of this bacterial genus is from the activated sludges of coking wastewater treatment plant, *Mycobacterium* shows ability to degrade PAHs. Other studies had reported the capability of genus *Mycobacterium* to transform a broad range of PAHs, including naphthalene, phenanthrene, fluoranthene, pyrene, and even five-ring benzo[*a*]pyrene (Kim et al. 2012; Zeng et al. 2017).

3.2 Degradation of Pyrene

Using pyrene as the unique carbon and energy source, CP13 could degrade pyrene with high efficiency. As shown in Fig. 2a ($p < 0.001$), the degradation efficiency of pyrene was more than 93% when initial concentration was less than 75 mg L^{-1}, and the highest pyrene degradation efficiency was found at 50 mg L^{-1}. However, the degradation percentages of pyrene decreased to 84% and 67% when initial pyrene concentrations raised to 100 and 150 mg L^{-1}, respectively. This phenomenon was probably attributed to the accumulation of toxic intermediate products when initial pyrene concentration was relevantly high, resulting in inhibition of microbial activity (Lu et al. 2013; Hadibarata et al. 2017).

Temperature and pH are two significant environmental parameters which can affect the degradation potential of microorganisms (Tao et al. 2007). Figure 2b ($p < 0.001$) showed that the optimal degradation temperature for CP13 was 35 °C, followed by 30 °C. However, the pyrene degradation percentages were significantly declined when temperature dropped to 25 °C or rose to 40 °C. Microorganisms that were cultivated at inappropriate temperature may result in the decrease of PAH biodegradation since temperature is considered to be directly related to the enzymatic activity (Mukherjee et al. 2017).

The highest degradation proportions were observed at pH 8.0 and 9.0 with more than 95% of total pyrene after 7-day cultivation (Fig. 2c, $p < 0.001$). This indicated that the preference of strain CP13 was alkaline condition, which is different from many other reported pyrene-degrading bacteria (shown in Table 1). It is reported that *Mycobacterium gilvum* PYR-GCK has a greater performance under a slightly acid environment, due to the increase of cell membrane permeability to substrates (Badejo et al. 2013a). However, strain CP13 is originated from activated sludge of a coking wastewater treatment plant, which enables it to adapt to the alkaline environment after a long-term stable operation within relatively high pH level (Zhang et al. 2012). Moreover, some acid compounds generated within the degradation process could be neutralized by OH^-, which might facilitate the biotransformation reaction.

The investigation of the influences of incubation conditions on pyrene biodegradation provides the possibility of strain CP13 to be applied under different scales of pyrene concentration, temperature, and pH

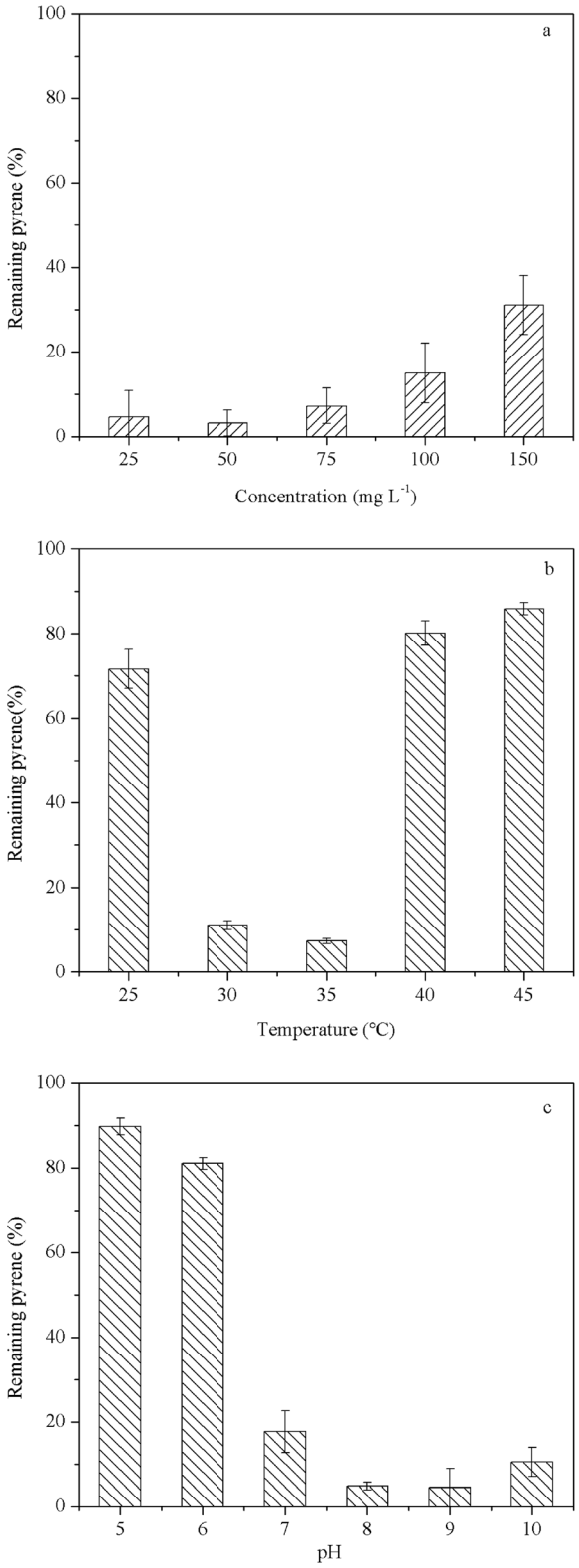

Fig. 2 Effects of different pyrene concentrations (**a**), temperatures (**b**), and pH values (**c**) on pyrene degradation. Data are represented as mean values ± standard errors

value. Comparison of incubation conditions and pyrene degradation efficiency of different bacterial species in previous reports are listed in Table 1. The degradation efficiency of CP13 is relatively higher than other reported bacterial strains. In addition, the phenomenon of pyrene degradation activity in alkaline condition suggests that CP13 may be more applicable to industrial wastewater treatments and/or contaminated field bioremediation which suffers from different degrees of alkalization with PAHs contamination.

3.3 Metabolites in Pyrene Biodegradation

Four intermediate products were observed during the process of pyrene degradation by CP13 (Table 2). Metabolite I displayed a molecular ion (M^+) at *m/z* 148 with a retention time of 11.19 min. The fragment ions at *m/z* 104 (M^+-44) and 76 (M^+-72) were attributed to loosing –COO and –CO, respectively. Thus, metabolite I was tentatively identified as phthalic acid. The loss of H_2O was probably due to the reaction between two carboxyl groups within phthalic acid. The metabolite II (*m/z* 144) was detected at 13.05 min and identified as 1-naphthol, which was in accord with the mass spectrum of an authentic standard. The remarkable fragment ion at *m/z* 115 (M^+-29) represented a loss of –CHO, and another fragment ion at *m/z* 89 (M^+-55) was relevant to the loss of –HC=CH–. Metabolite III, with a molecular ion (M^+) at *m/z* 194, was detected at retention time of 19.68 min. The mass spectrum revealed a major fragment ion at *m/z* 165 (M^+-29) and another fragment ion at *m/z* 139 (M^+-55), corresponding to the loss of –CHO and –HC=CH–, respectively. According to the mass spectrum, metabolite III was suggested to be 4-phenanthrenol. Metabolite IV was observed at 20.90 min (retention time) and suggested to be 4-phenanthrenecarboxylic acid. The molecular ion (M^+) of metabolite IV was *m/z* 222, and the fragment ions was *m/z* 176 (M^+-46), indicating the loss of –COOH and H.

Mycobacterium gilvum CP13 was cultivated under alkaline condition, and the four characterized metabolites were commonly presented in other studies of pyrene-degrading microorganisms (Jin et al. 2016; Kweon et al. 2014). The detection result of metabolites suggests that pyrene was primarily attacked at positions

Table 2 Metabolites detected by GC-MS during pyrene degradation

Metabolites	RT (min)	*m/z* of fragments ions (% relative abundance)	Metabolites structural suggestion
I	11.17	148(M^+,17),104(100), 76(53)	Phthalic acid
II	13.05	144(M^+,100), 115(76), 89(17), 83(21)	1-Naphthol
III	19.68	194(M^+,100), 165(99), 139(10), 82(18)	4-Phenanthrenol
IV	20.90	222(M^+,100), 176(8), 110(16)	4-Phenanthrenecarboxylic acid

C-4 and C-5, and then after *ortho* cleavage and decarboxylation, 4-phenanthrenecarboxylic acid was formed and then transformed to 4-phenanthrenol. Also, 4-phenanthrenecarboxylic acid could be further degraded to 1-naphthol which was subsequently decomposed to phthalate acid (Fig. 3). This study is similar to the result of alkaliphilic *Mycobacterium* sp. strain MHP-1 as reported by Habe et al. (2004) and consisted with the essential feature of major pyrene degradation pathway as well (Liang et al. 2006; Krivobok et al. 2003; Kim et al. 2007; Seo et al. 2011; Kweon et al. 2011).

Mycobacterium, a Gram-positive genera, has been broadly studied because of its versatility in PAH degradation (Seo et al. 2009). For example, it is found that *Mycobacterium flavescens*, *Mycobacterium* sp. strain KR2, and *Mycobacterium* sp. strain AP1 can transform pyrene into *cis*-4,5-pyrenedihydrodiol or *trans*-4,5-pyrenedihydrodiol with initial attack on the positions of C-4 and C-5 (Dean-Ross and Cerniglia 1996; Rehmann et al. 1998; Vila et al. 2001). Moreover, both *Mycobacterium vanbaalenii* PYR-1 and *Mycobacterium* sp. strain A1-PYR can firstly oxidize pyrene not only on the positions of C-4 and C-5, but also on the positions of C-1 and C-2 (Zhong et al. 2006; Kim et al. 2005). However, a dead end product, 4-hydroxyperinaphthenone, was found within the metabolic pathway of *Mycobacterium vanbaalenii* PYR-1 (Kim et al. 2005).

In some cases, PAH biodegradation is an incomplete process that result in the accumulation of intermediate products. Some intermediate products (e.g., arene oxides, phenols, and dihydrodiols) have been classified as carcinogenic and mutagenic matters, and they pose more significant risks to the ecosystems than their parent compounds because of the increase in solubility and mobility (Tiwari et al. 2010). In this study, 4-phenanthrenol is considered to be the dead-end product within the degradation pathway; however, whether its accumulation has adverse effects on cell growth or degradation process deserves to have a further study.

3.4 Analysis and Identification of Proteins

The study of proteins/enzymes involved in PAHs biodegradation would provide a better way to understand the responses of microorganisms to the environmental conditions (Chauhan and Jain 2010; Mukherjee et al. 2017). The total soluble proteins were extracted from strain CP13 and isolated by 2-DE. As a whole, the spot patterns were reproducible through different samples, and dozens of distinct polypeptide spots were visualized by silver stains (Fig. 4). The spot numbers and densities varied with different substrates and pH values. In comparison with the sorbitol-treated sample, certain proteins induced by pyrene were up-regulated more than two folds: six proteins enhanced and four newly synthesized in pH 7 condition; ten proteins enhanced and three newly synthesized in pH 9 condition (Table 3). In addition, among the identified proteins, those of pyrene-induced sample at pH 9 showed different spot intensities from those of pyrene-induced sample at pH 7 (eight proteins enhanced, nine down-regulated, and one newly synthesized), indicating that microorganisms would produce corresponding proteins to meet the physiological needs under different external environments.

Eighteen proteins of interest were identified by Mascot search within the existing database, and the corresponding information is displayed in Table 3. Functions of some identified proteins are missing, owing to the lack of relevant references and researches. Sports 4, 7, and 13 were matched with proteins related to DNA binding, i.e., periplasmic binding s and sugar binding domain of the LacI family protein, DNA/RNA helicase, and Gp47, respectively. Spot 5 was identified as translation elongation factor 1A (EF-1A/EF-Tu), involving in GTPase activity. Spot 8, identified as glycosyl transferase group1, was associated with catalysis of glycosyl group transfer. Spot 10 was identified as glucose-methanol-choline oxidoreductase, relevant to glucose and choline oxidoreduction activities, acting on CH-OH group of donors. Spot 18 was identified as putative

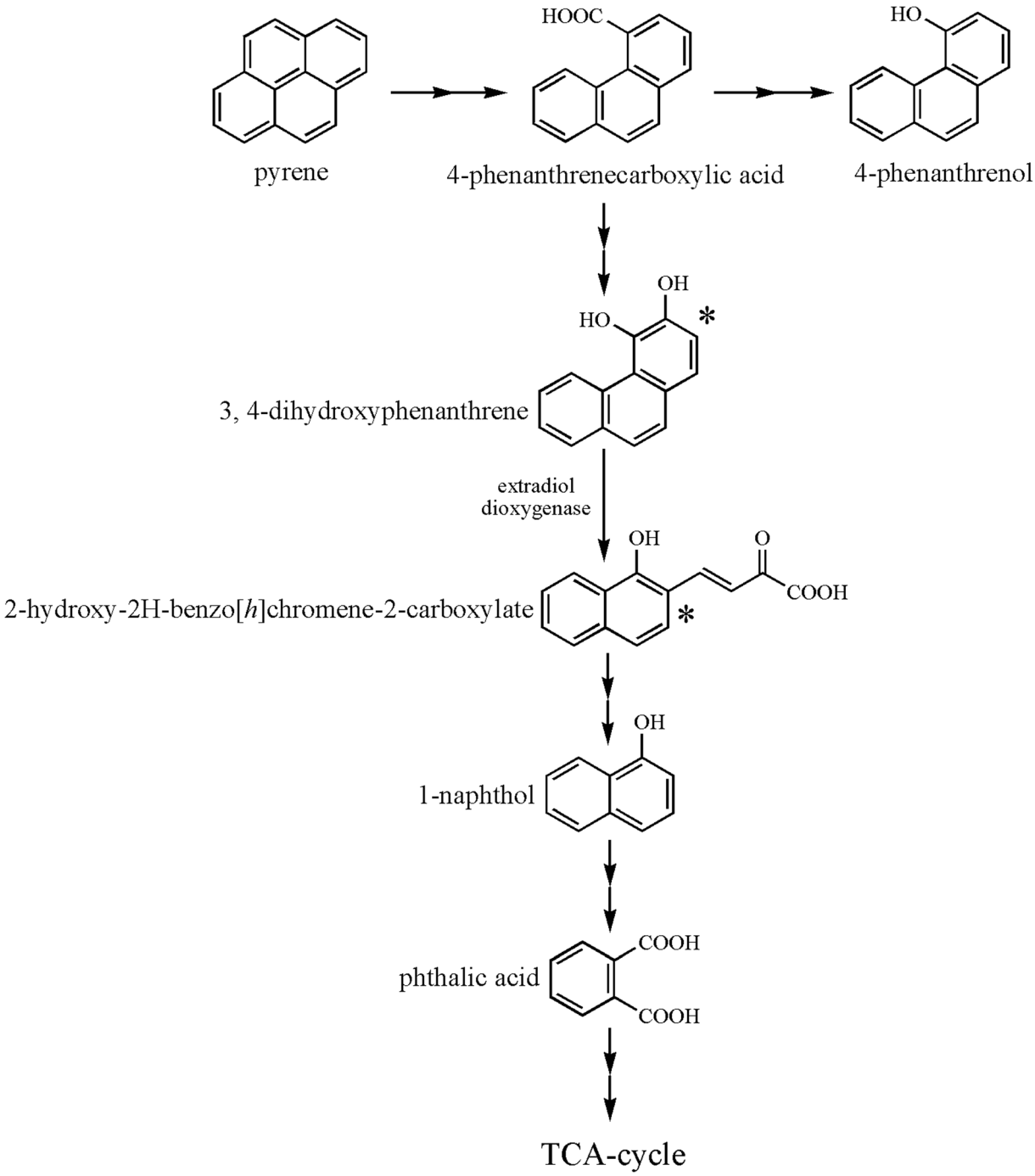

Fig. 3 Proposed degradation pathway of pyrene by stain CP13 (The single arrows indicate one step and the double arrows represent multiple steps. Metabolites with asterisks have not been detected)

extradiol dioxygenase, coded by gene *phdF*, participating in the catabolism of aromatic compounds.

As for genus *Mycobacterium*, the enzymatic mechanism of PAHs degradation has been widely investigated, and dioxygenases involved in aromatic ring oxidation are the key enzymes according to the previous reports. For example, dioxygenases Pdo1 and Pdo2, originated from *Mycobacterium* sp. strain 6PY1, were suggested to

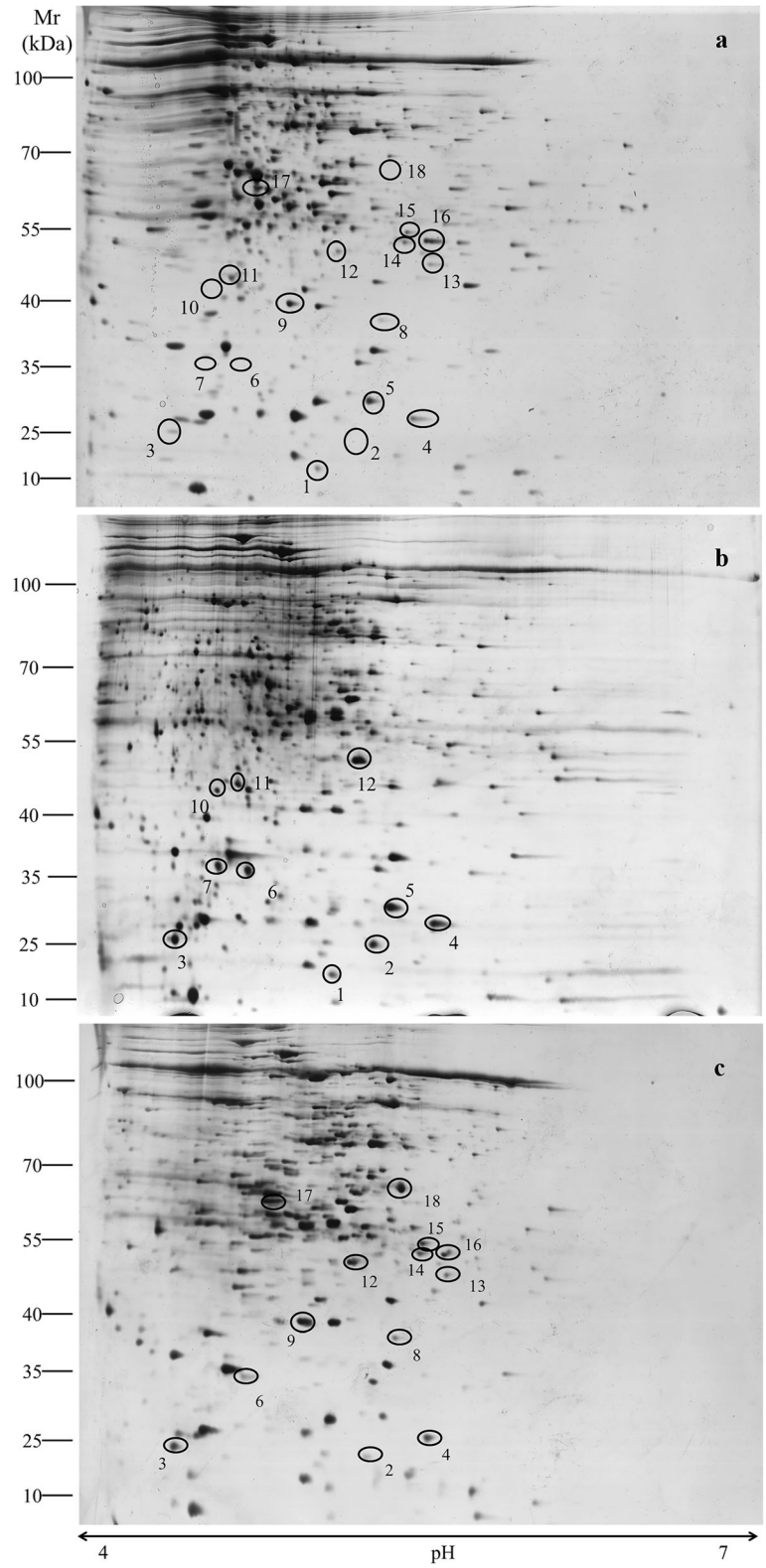

Fig. 4 2-DE images of the total soluble proteins extracted from strain CP13 grown with sorbitol (**a**) and pyrene (**b** (pH 7) and **c** (pH 9))

Table 3 Identification of up-regulated proteins of CP13 grown in two pH conditions

Spot no.	Protein name	p*I* [a]	Approx. fold change[b]		Microorganism	NCBI GI no.	Function
			pH 7	pH 9			
1	RES domain-containing protein	5.16	2.01	1.10	*Mycobacterium smegmatis* JS623	gi|433644573	Unknown
2	Hypothetical protein	5.32	∞	∞	*Mycobacterium smegmatis*	gi|489991805	Unknown
3	Gp117	4.51	11.54	7.49	*Mycobacterium phage Optimus*	gi|339752138	Unknown
4	Periplasmic binding s and sugar binding domain of the LacI family protein	5.59	2.1	2.76	*Mycobacterium smegmatis* strain MKD8	gi|489994386	DNA binding, regulation of transcription
5	Translation elongation factor 1A (EF-1A/EF-Tu)	5.39	2.15	0.73	*Mycobacterium smegmatis* JS623	gi|433295582	GTPase activity, nucleotide binding, translation elongation, GTP binding
6	Gp47	4.77	∞	∞	*Mycobacterium phage Zemanar*	gi|339755717	Unknown
7	DNA/RNA helicase, superfamily II, SNF2 family	4.59	∞	–	*Mycobacterium smegmatis* JS623	gi|433644703	DNA binding, ATP binding, helicase activity, hydrolase activity
8	Glycosyl transferase group1	5.44	1.83	3.48	*Mycobacterium smegmatis* strain MC2 155	gi|399990169	Transferase activity
9	RES domain-containing protein	5.03	1.67	2.02	*Mycobacterium smegmatis* JS623	gi|433644573	Unknown
10	Glucose-methanol-choline oxidoreductase	4.62	∞	–	*Mycobacterium smegmatis* strain MC2 155	gi|118174675	Flavin adenine dinucleotide binding, oxidoreductase activity, acting on CH-OH group of donors, oxidation- reduction process
11	Gp117	4.77	3.15	1.58	*Mycobacterium phage Optimus*	gi|339752138	Unknown
12	Hypothetical protein	5.25	11.22	4.76	*Mycobacterium smegmatis*	gi|489989134	Unknown
13	Gp47	5.67	0.16	4.15	*Mycobacterium phage Spartacus*	gi|375281881	DNA binding
14	Gp52	5.55	0.55	2.75	*Mycobacterium phage Konstantine*	gi|206600035	Unknown
15	Hypothetical protein WIVsmall_32	5.56	0.19	3.26	*Mycobacterium phage WIVsmall*	gi|485727204	Unknown
16	Gp94	5.65	1.08	3.66	*Mycobacterium phage Marvin*	gi|339755367	Unknown
17	RES domain-containing protein	4.89	0.40	2.35	*Mycobacterium smegmatis* JS623	gi|433644573	Unknown
18	Putative extradiol dioxygenase, *phdF*	5.46	–	∞	*Mycobacterium* sp. SNP11	gi|116805451	Catalytic activity, dioxygenase activity, ferrous iron binding, oxidoreductase activity, aromatic compound catabolic process

[a] p*I* was estimated from data in Fig. 4

[b] Average values from duplicate experiments. Spot density compared with the control: ∞/— indicates the protein was newly detected/not observed on the gel

convert pyrene into pyrene cis-4,5-dihydrodiol and actively involved in the catabolism of phenanthrene, respectively (Krivobok et al. 2003). In addition, it is reported that pyrene was metabolized by *Mycobacterium vanbaalenii* PYR-1 with both monooxygenase and dioxygenase (Kim et al. 2004). Further study on *Mycobacterium vanbaalenii* PYR-1 employed both proteomic and genomic approaches, in

which 18 up-regulated enzymes (over twofold) were identified, such as ring-cleavage dioxygenase (MvanDraft_3242), dihydrodiol dehydrogenase (MvanDraft_0815), and ring-hydroxylating oxygenase (MvanDraft_0817/0818) (Kim et al. 2007).

The up-regulated proteins in this study are associated with different cellular functions, such as DNA condensation (spot 4, 7, and 13), transferring activity (spot 8), translation (spot 5), metabolism (spot 18), and other redox reaction (spot 10). Even though the proteins at low copy level or insoluble could not be presented by 2-DE, this proteomic approach provides a better insight into the protein separation and comparison (Kim et al. 2004). Here, proteins with different functions are considered to be directly/indirectly related to the enhancement of pyrene degradation under given conditions. Interestingly, Spot 18 (putative extradiol dioxygenase) was newly synthesized in pH 9 condition with pyrene induced, supporting CP13 in pyrene degradation under alkaline environment. According to the previous reports, extradiol dioxygenase has been suggested to be involved in the transformation of 3,4-dihydroxyphenanthrene to its fewer ringed carboxylate intermediate products (i.e., 2-hydroxy-2H-benzo[*h*]chromene-2-carboxylate) (Badejo et al. 2013a; Kim et al. 2007; Krivobok et al. 2003). The up-regulation of extradiol dioxygenase may be the reason that strain CP13 maintains high efficiency under alkaline environment. However, other enzymes associated with pyrene catabolism (e.g., ring-hydroxylting dioxygenase, dihydrodiol dioxygenase, decarboxylase) were not detected in this study, probably because of the low expression level that required to be further confirmed by a study of genomic sequence analysis of CP13.

4 Conclusions

This study shows that *Mycobacterium gilvum* strain CP13 isolated from activated sludge can effectively degrade over 95% of pyrene (50 mg L^{-1}) under alkaline condition (pH 8–9). During pyrene biodegradation process, four metabolites (i.e., phthalic acid, 1-naphthol, 4-phenanthrenol, and 4-phenanthrenecarboxylic acid) as well as some pyrene-induced proteins were identified. Proteins, such as translation elongation factor 1A (EF-1A/EF-Tu), glycosyl transferase group 1, and glucose-methanol-choline oxidoreductase, associated with different cellular functions were involved in pyrene biodegradation. Moreover, a PAH-related enzyme, extradiol dioxygenase, was significantly up-regulated in the pH 9 incubation condition, enabling CP13 to maintain high efficiency under alkaline environment. This study focusses on investigating the pyrene-induced proteins in alkaline condition by genus *Mycobacterium*, which also gives a basic understanding of pyrene degradation metabolism of CP13, suggesting that CP13 could be a representative bacterial strain for application in PAH bioremediation under alkaline condition.

Funding Information This work was supported by the Guangdong Provincial Science and Technology Projects (2014A020217002 and 2016B020242004).

References

Badejo, A. C., Badejo, A. O., Shin, K. H., & Chai, Y. G. (2013a). A gene expression study of the activities of aromatic ring-cleavage dioxygenases in *Mycobacterium gilvum* PYR-GCK to changes in salinity and pH during pyrene degradation. *PLoS One, 8*(2), e58066. https://doi.org/10.1371/journal.pone.0058066.

Badejo, A. C., Choi, C. W., Badejo, A. O., Shin, K. H., Hyun, J. H., Lee, Y. G., et al. (2013b). A global proteome study of *Mycobacterium gilvum* PYR-GCK grown on pyrene and glucose reveals the activation of glyoxylate, shikimate and gluconeogenetic pathways through the central carbon metabolism highway. *Biodegradation, 24*(6), 741–752. https://doi.org/10.1007/s10532-013-9622-9.

Balcom, I. N., & Crowley, D. E. (2010). Isolation and characterization of pyrene metabolizing microbial consortia from the plant rhizoplane. *International Journal of Phytoremediation, 12*(6), 599–615. https://doi.org/10.1080/15226510903390437.

Chauhan, A., & Jain, R. K. (2010). Biodegradation: Gaining insight through proteomics. *Biodegradation, 21*(6), 861–879. https://doi.org/10.1007/s10532-010-9361-0.

Chebbi, A., Hentati, D., Zaghden, H., Baccar, N., Rezgui, F., Chalbi, M., et al. (2017). Polycyclic aromatic hydrocarbon degradation and biosurfactant production by a newly isolated *Pseudomonas* sp. strain from used motor oil-contaminated soil. *International Biodeterioration & Biodegradation, 122*, 128–140. https://doi.org/10.1016/j.ibiod.2017.05.006.

Chen, J., Aries, E., Collins, P., Anderson, D. R., & Hodges, J. S. (2015). Characterization of priority substances in effluents

from an integrated steelworks in the United Kingdom. *Water Environment Research, 87*(2), 132–144. https://doi.org/10.2175/106143014X14062131179311.

Dean-Ross, D., & Cerniglia, C. E. (1996). Degradation of pyrene by *Mycobacterium flavescens*. *Applied Microbiology and Biotechnology, 46*(3), 307–312.

Guo, C. L., Dang, Z., Wong, Y. S., & Tam, N. F. (2010). Biodegradation ability and dioxgenase genes of PAH-degrading *Sphingomonas* and *Mycobacterium* strains isolated from mangrove sediments. *International Biodeterioration & Biodegradation, 64*(6), 419–426. https://doi.org/10.1016/j.ibiod.2010.04.008.

Habe, H., Kanemitsu, M., Nomura, M., Takemura, T., Iwata, K., Nojiri, H., et al. (2004). Isolation and characterization of an alkaliphilic bacterium utilizing pyrene as a carbon source. *Journal of Bioscience and Bioengineering, 98*(4), 306–308. https://doi.org/10.1263/Jbb.98.306.

Hadibarata, T., Khudhair, A. B., Kristanti, R. A., & Kamyab, H. (2017). Biodegradation of pyrene by *Candida* sp. S1 under high salinity conditions. *Bioprocess and Biosystems Engineering, 40*, 1411–1418. https://doi.org/10.1007/s00449-017-1798-7.

Hilyard, E. J., Jones-Meehan, J. M., Spargo, B. J., & Hill, R. T. (2008). Enrichment, isolation, and phylogenetic identification of polycyclic aromatic hydrocarbon-degrading bacteria from Elizabeth River sediments. *Applied and Environmental Microbiology, 74*(4), 1176–1182. https://doi.org/10.1128/Aem.01518-07.

Jin, J. N., Yao, J., Zhang, Q. Y., & Liu, J. L. (2016). Biodegradation of pyrene by *pseudomonas* sp. JPN2 and its initial degrading mechanism study by combining the catabolic *nahAc* gene and structure-based analyses. *Chemosphere, 164*, 379–386. https://doi.org/10.1016/j.chemosphere.2016.08.113.

Kim, S. J., Jones, R. C., Cha, C. J., Kweon, O., Edmondson, R. D., & Cerniglia, C. E. (2004). Identification of proteins induced by polycyclic aromatic hydrocarbon in *Mycobacterium vanbaalenii* PYR-1 using two-dimensional polyacrylamide gel electrophoresis and de novo sequencing methods. *Proteomics, 4*(12), 3899–3908. https://doi.org/10.1002/pmic.200400872.

Kim, Y. H., Freeman, J. P., Moody, J. D., Engesser, K. H., & Cerniglia, C. E. (2005). Effects of pH on the degradation of phenanthrene and pyrene by *Mycobacterium vanbaalenii* PYR-1. *Applied Microbiology and Biotechnology, 67*(2), 275–285. https://doi.org/10.1007/s00253-004-1796-y.

Kim, S. J., Kweon, O., Jones, R. C., Freeman, J. P., Edmondson, R. D., & Cerniglia, C. E. (2007). Complete and integrated pyrene degradation pathway in *Mycobacterium vanbaalenii* PYR-1 based on systems biology. *Journal of Bacteriology, 189*(2), 464–472. https://doi.org/10.1128/Jb.01310-06.

Kim, S. J., Song, J., Kweon, O., Holland, R. D., Kim, D. W., Kim, J., et al. (2012). Functional robustness of a polycyclic aromatic hydrocarbon metabolic network examined in a *nidA* aromatic ring-hydroxylating oxygenase mutant of *Mycobacterium vanbaalenii* PYR-1. *Applied and Environmental Microbiology, 78*(10), 3715–3723. https://doi.org/10.1128/Aem.07798-11.

Kristanti, R. A., Hadibarata, T., Al Farraj, D. A., Elshikh, M. S., & Alkufeidy, R. M. (2018). Biodegradation mechanism of phenanthrene by *Halophilic Hortaea* sp B15. *Water, Air, and Soil Pollution, 229*(10). https://doi.org/10.1007/s11270-018-3969-9.

Krivobok, S., Kuony, S., Meyer, C., Louwagie, M., Willison, J. C., & Jouanneau, Y. (2003). Identification of pyrene-induced proteins in *Mycobacterium sp.* strain 6PY1: Evidence for two ring-hydroxylating dioxygenases. *Journal of Bacteriology, 185*(13), 3828–3841. https://doi.org/10.1128/Jb.185.13.3828.3841.2003.

Kumari, S., Regar, R. K., & Manickam, N. (2018). Improved polycyclic aromatic hydrocarbon degradation in a crude oil by individual and a consortium of bacteria. *Bioresource Technology, 254*, 174–179. https://doi.org/10.1016/j.biortech.2018.01.075.

Kweon, O., Kim, S. J., Holland, R. D., Chen, H. Y., Kim, D. W., Gao, Y., et al. (2011). Polycyclic aromatic hydrocarbon metabolic network in *Mycobacterium vanbaalenii* PYR-1. *Journal of Bacteriology, 193*(17), 4326–4337. https://doi.org/10.1128/Jb.00215-11.

Kweon, O., Kim, S. J., Kim, D. W., Kim, J. M., Kim, H. L., Ahn, Y., et al. (2014). Pleiotropic and epistatic behavior of a ring-hydroxylating oxygenase system in the polycyclic aromatic hydrocarbon metabolic network from *Mycobacterium vanbaalenii* PYR-1. *Journal of Bacteriology, 196*(19), 3503–3515. https://doi.org/10.1128/Jb.01945-14.

Liang, Y., Gardner, D. R., Miller, C. D., Chen, D., Anderson, A. J., Weimer, B. C., et al. (2006). Study of biochemical pathways and enzymes involved in pyrene degradation by *Mycobacterium* sp. strain KMS. *Applied and Environmental Microbiology, 72*(12), 7821–7828. https://doi.org/10.1128/Aem.01274-06.

Ling, J. Y., Zhang, G. Y., Sun, H. B., Fan, Y. Y., Ju, J. H., & Zhang, C. K. (2011). Isolation and characterization of a novel pyrene-degrading *Bacillus vallismortis* strain JY3A. *Science of the Total Environment, 409*(10), 1994–2000. https://doi.org/10.1016/j.scitotenv.2011.02.020.

Liu, S. S., Guo, C. L., Liang, X. J., Wu, F. J., & Dang, Z. (2016). Nonionic surfactants induced changes in cell characteristics and phenanthrene degradation ability of *Sphingomonas* sp. GY2B. *Ecotoxicology and Environmental Safety, 129*, 210–218. https://doi.org/10.1016/j.ecoenv.2016.03.035.

Liu, S. S., Guo, C. L., Dang, Z., & Liang, X. J. (2017). Comparative proteomics reveal the mechanism of Tween80 enhanced phenanthrene biodegradation by *Sphingomonas* sp. GY2B. *Ecotoxicology and Environmental Safety, 137*, 256–264. https://doi.org/10.1016/j.ecoenv.2016.12.015.

Lu, J., Guo, C. L., Li, J., Zhang, H., Lu, G. N., Dang, Z., et al. (2013). A fusant of *Sphingomonas* sp. GY2B and *Pseudomonas* sp. GP3A with high capacity of degrading phenanthrene. *World Journal of Microbiology and Biotechnology, 29*(9), 1685–1694. https://doi.org/10.1007/s11274-013-1331-3.

Mukherjee, A. K., Bhagowati, P., Biswa, B. B., Chanda, A., & Kalita, B. (2017). A comparative intracellular proteomic profiling of *Pseudomonas aeruginosa* strain ASP-53 grown on pyrene or glucose as sole source of carbon and identification of some key enzymes of pyrene biodegradation pathway. *Journal of Proteomics, 167*, 25–35. https://doi.org/10.1016/j.jprot.2017.07.020.

Ping, L. F., Zhang, C. R., Zhang, C. P., Zhu, Y. H., He, H. M., Wu, M., et al. (2014). Isolation and characterization of pyrene and benzo[a]pyrene-degrading *Klebsiella pneumonia* PL1 and its

potential use in bioremediation. *Applied Microbiology and Biotechnology, 98*(8), 3819–3828. https://doi.org/10.1007/s00253-013-5469-6.

Ping, L. F., Zhang, C. R., Cui, H., Yuan, X. L., Cui, J. T., & Shan, S. D. (2017). Characterization and application of a newly isolated pyrene-degrading bacterium, *Pseudomonas monteilii*. *3 Biotech, 7*, 309. https://doi.org/10.1007/S13205-017-0945-9.

Rehmann, K., Noll, H. P., Steinberg, C. E., & Kettrup, A. A. (1998). Pyrene degradation by *Mycobacterium* sp. strain KR2. *Chemosphere, 36*(14), 2977–2992.

Seo, J. S., Keum, Y. S., & Li, Q. X. (2009). Bacterial degradation of aromatic compounds. *International Journal of Environmental Research and Public Health, 6*(1), 278–309. https://doi.org/10.3390/ijerph6010278.

Seo, J. S., Keum, Y. S., & Li, Q. X. (2011). Comparative protein and metabolite profiling revealed a metabolic network in response to multiple environmental contaminants in *Mycobacterium aromativorans* JS19b1(T). *Journal of Agricultural and Food Chemistry, 59*(7), 2876–2882. https://doi.org/10.1021/jf103018s.

Smol, M., & Wlodarczyk-Makula, M. (2012). Effectiveness in the removal of polycyclic aromatic hydrocarbons from industrial wastewater by ultrafiltration technique. *Archives of Environmental Protection, 38*(4), 49–58. https://doi.org/10.2478/v10265-012-0040-6.

Tao, X. Q., Lu, G. N., Dang, Z., Yang, C., & Yi, X. Y. (2007). A phenanthrene-degrading strain *Sphingomonas* sp. GY2B isolated from contaminated soils. *Process Biochemistry, 42*(3), 401–408. https://doi.org/10.1016/j.procbio.2006.09.018.

Tiwari, J. N., Reddy, M. M. K., Patel, D. K., Jain, S. K., Murthy, R. C., & Manickam, N. (2010). Isolation of pyrene degrading *Achromobacter xylooxidans* and characterization of metabolic product. *World Journal of Microbiology and Biotechnology, 26*(10), 1727–1733. https://doi.org/10.1007/s11274-010-0350-6.

Vila, J., Lopez, Z., Sabate, J., Minguillon, C., Solanas, A. M., & Grifoll, M. (2001). Identification of a novel metabolite in the degradation of pyrene by *Mycobacterium* sp. strain AP1: Actions of the isolate on two- and three-ring polycyclic aromatic hydrocarbons. *Applied and Environmental Microbiology, 67*(12), 5497–5505. https://doi.org/10.1128/Aem.67.12.5497-5505.2001.

Wongwongsee, W., Chareanpat, P., & Pinyakong, O. (2013). Abilities and genes for PAH biodegradation of bacteria isolated from mangrove sediments from the central of Thailand. *Marine Pollution Bulletin, 74*(1), 95–104. https://doi.org/10.1016/Imarpolbu1.2013.07.025.

Yan, Z. S., Zhang, Y., Wu, H. F., Yang, M. Z., Zhang, H. C., Hao, Z. C., et al. (2017). Isolation and characterization of a bacterial strain *Hydrogenophaga* sp. PYR1 for anaerobic pyrene and benzo[a]pyrene biodegradation. *RSC Advances, 7*(74), 46690–46698. https://doi.org/10.1039/c7ra09274a.

Yuan, H. Y., Yao, J., Masakorala, K., Wang, F., Cai, M. M., & Yu, C. (2014). Isolation and characterization of a newly isolated pyrene-degrading *Acinetobacter* strain USTB-X. *Environmental Science and Pollution Research, 21*(4), 2724–2732. https://doi.org/10.1007/s11356-013-2221-9.

Zeng, J., Zhu, Q. H., Wu, Y. C., Chen, H., & Lin, X. G. (2017). Characterization of a polycyclic aromatic ring-hydroxylation dioxygenase from *Mycobacterium* sp. NJS-P. *Chemosphere, 185*, 67–74. https://doi.org/10.1016/j.chemosphere.2017.07.001.

Zhang, M., & Zhu, L. (2009). Sorption of polycyclic aromatic hydrocarbons to carbohydrates and lipids of ryegrass root and implications for a sorption prediction model. *Environmental Science & Technology, 43*(8), 2740–2745. https://doi.org/10.1021/es802808q.

Zhang, W. H., Wei, C. H., Chai, X. S., He, J. Y., Cai, Y., Ren, M., et al. (2012). The behaviors and fate of polycyclic aromatic hydrocarbons (PAHs) in a coking wastewater treatment plant. *Chemosphere, 88*(2), 174–182. https://doi.org/10.1016/j.chemosphere.2012.02.076.

Zhang, J., Yang, J. C., Wang, R. Q., Hou, H., Du, X. M., Fan, S. K., et al. (2013). Effects of pollution sources and soil properties on distribution of polycyclic aromatic hydrocarbons and risk assessment. *Science of the Total Environment, 463*, 1–10. https://doi.org/10.1016/j.scitotenv.2013.05.066.

Zhong, Y., Luan, T. G., Zhou, H. W., Lan, C. Y., & Tam, N. F. Y. (2006). Metabolite production in degradation of pyrene alone or in a mixture with another polycyclic aromatic hydrocarbon by *Mycobacterium* sp. *Environmental Toxicology and Chemistry, 25*(11), 2853–2859. https://doi.org/10.1897/06-042r.1.

Zhou, H. Y., Wang, H., Huang, Y., & Fang, T. T. (2016). Characterization of pyrene degradation by halophilic *Thalassospira* sp. strain TSL5-1 isolated from the coastal soil of Yellow Sea, China. *International Biodeterioration & Biodegradation, 107*, 62–69. https://doi.org/10.1016/j.ibiod.2015.10.022.